ResearchGate

See discussions, stats, and author profiles for this publication at: https://www.researchgate.net/publication/231661560

Characterization of the (D2O)2 Hydrogen-Bond-Acceptor Antisymmetric Stretch by IR Cavity Ringdown Laser Absorption Spectroscopy

ARTICLE *in* THE JOURNAL OF PHYSICAL CHEMISTRY A · APRIL 1998

Impact Factor: 2.69 · DOI: 10.1021/jp980763x

CITATIONS
49

READS
16

3 AUTHORS, INCLUDING:

Robert Provencal
Los Gatos Research
44 PUBLICATIONS **1,009** CITATIONS
SEE PROFILE

Richard J Saykally
University of California, Berkeley
460 PUBLICATIONS **28,045** CITATIONS
SEE PROFILE

Available from: Robert Provencal
Retrieved on: 16 January 2016

Characterization of the $(D_2O)_2$ Hydrogen-Bond-Acceptor Antisymmetric Stretch by IR Cavity Ringdown Laser Absorption Spectroscopy

J. B. Paul, R. A. Provencal, and R. J. Saykally*

Department of Chemistry, University of California, Berkeley, California 94720

Received: January 13, 1998; In Final Form: March 10, 1998

The IR-CRLAS technique has been used to measure the mid-infrared O−D stretching spectrum of the fully deuterated gas-phase water dimer for the first time. The instrumentally limited resolution of 1 GHz resolves the acceptor tunneling splittings and the rotational line manifolds. The analysis of these splittings exploits the local nature of the excitation and yields a description of the acceptor tunneling motion that supports previous experimental and theoretical results.

Introduction

The study of water clusters is currently the focus of considerable theoretical and experimental activity. New infrared and far-IR spectroscopic methods have revealed a wealth of detail regarding structures, hydrogen-bond tunneling dynamics, and intermolecular vibrational motions in water clusters as large as the octamer.[1−3] Ab initio calculations have provided much insight into the intermolecular potential energy surfaces (IPS) governing their properties,[4] and new dynamical techniques[5,6] have made it possible to interpret the high-resolution spectra of these clusters directly in terms of the many-body dynamics occurring on the IPS.

One of the principal motivations for these investigations is to extract an improved intermolecuar force field for liquid and solid water by systematically untangling the complex many-body interactions that plague theoretical treatments of the condensed phases.[1,2,6] The first step in this scenario is to determine a precise water−water pair potential from a regression analysis of the spectroscopic data available for the water dimer, constrained by ab initio calculations.[7] Initially, this will necessarily proceed within a frozen monomer (6-D) analysis, but ultimately one wishes to quantify the monomer relaxation that accompanies hydrogen-bond formation.[6] This will require a detailed knowledge of the coupling between inter- and intramolecular motions in the dimer, such as is obtained from high-resolution mid-IR spectroscopy of the chemical bonds in water clusters. To further advance such knowledge is the purpose of the work described herein.

The O−H stretching vibrations in water clusters have been investigated quite extensively in the 2−3 μm spectral region, but only by indirect spectroscopic methods (vibrational predissociation,[8−10] bolometric detection[11,12]) or cryogenic matrix spectroscopy,[13−15] until our recent IR cavity ringdown laser absorption spectroscopy (CRLAS) study.[16] To the best of our knowledge, the corresponding gas-phase O−D stretches (3.5−4.5 μm) have not been observed previously, primarily because of the lack of suitable radiation sources in this spectral region. The use of cavity ringdown detection[17] greatly relaxes the demands on the light source, and a Raman-shifted pulsed dye laser conveniently provides complete coverage over these wavelengths. In this article we report the measurement and analysis of the hydrogen-bond acceptor antisymmetric O−D stretch in the $(D_2O)_2$ isotopomer. In addition to this band system, we have measured two other bands belonging to the fully deuterated dimer. These are both parallel band systems exhibiting considerable spectral congestion, making the rotational line assignments difficult. These bands, along with absorption features attributable to larger clusters, will be the subject of a future publication.

The $(H_2O)_2$ band analogous to that discussed here was first measured with rotational-tunneling resolution in 1989 by Huang and Miller.[11] Their work, along with extensive studies of the ground and low-lying vibrational states of both the normal and deuterated forms of the dimer compiled through far-infrared,[18−20] microwave,[21−23] and theoretical[20,24−26] studies, provides the foundation for our analysis of the new spectra presented here. It is presently accepted that large-amplitude motions involving the hydrogen bond facilitate tunneling between 16 symmetrically equivalent molecular frameworks, assuming that no chemical bonds are broken (eight if a plane of symmetry exists). Quantum tunneling among the associated minima on the 16-fold degenerate potential energy surface occurs primarily via three pathways, each involving relatively little O atom motion.[5]

The lowest barrier motion ($\sim$0.59 kcal mol^{-1}),[27] and the only one that does not require breaking the hydrogen bond, is commonly called "acceptor tunneling", as the overall result of this motion is the permutation of the acceptor hydrogen atoms. While a simple rotation of the acceptor monomer about the acceptor $\hat{c}_2$ axis is the most obvious pathway to this end, experimental and theoretical results imply that this motion actually consists of a concerted ammonia-like inversion of the proton acceptor molecule with a 180° torsional rotation of the donor molecule (Figure 1), similar to that of a well-studied tunneling motion in methylamine. The signature of these tunneling motions in the spectra will arise through the coupling of the angular momentum generated by the tunneling motion to the overall rotation of the cluster, and clearly these alternative pathways will generate significantly different amounts of angular momentum. Typically, this coupling produces a *K*-dependent splitting pattern which can be well-approximated by a cosine function.[28] As the selection rules do not allow direct transitions between these branches for the water dimer, the exact values for these splittings have not been determined. However, far-IR measurements of transitions between ground-state K_a levels of the H_2O dimer fit to expressions derived within the local-

S1089-5639(98)00763-4 CCC: $15.00 © 1998 American Chemical Society
Published on Web 04/17/1998

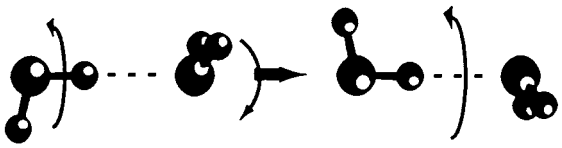

Figure 1. The lowest barrier tunneling pathway in the water dimer. This motion is commonly referred to as "acceptor tunneling", because the end result is the exchange of the hydrogen atoms of the hydrogen-bond acceptor monomer.

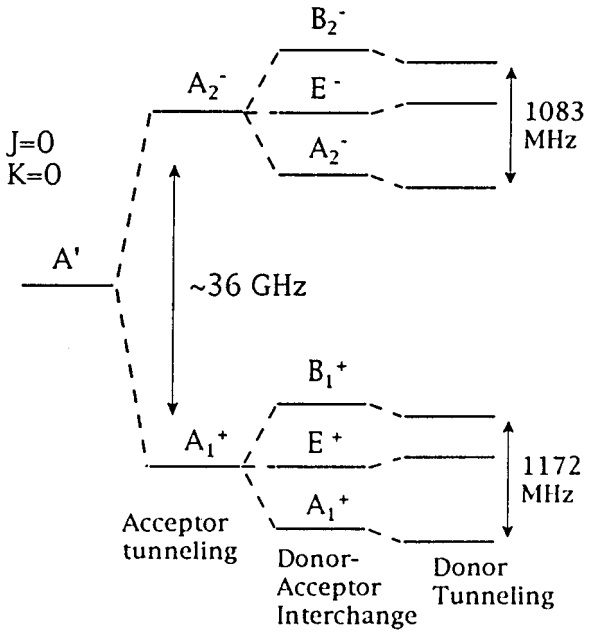

Figure 2. Energy level diagram of the $J = 0$, $K = 0$ ground state of $(D_2O)_2$. Each energy level of the rigid dimer is split into six components by various tunneling interactions.

IAM framework of Coudert and Hougen suggest that the splitting in $K_a'' = 0$ is 9.4 cm^{-1}. For the case of the D_2O dimer, the sum of the ground-state $K_a = 0$ and 1 splittings is measured to be 72 GHz. From this, the $K_a = 0$ splitting has been estimated to be 36 GHz.[21]

The remaining tunneling pathways include the exchange of the roles of the H-bond donor and acceptor monomers ("donor−acceptor interchange"), and a motion somewhat analogous to acceptor tunneling ("donor tunneling"), involving the exchange of the bound and free H's on the donor subunit. These remove all degeneracies resulting from permutation−inversion symmetry in the rigid dimer, further splitting each acceptor tunneling level into three components (six total) with the outer two levels being singly degenerate and the middle level doubly degenerate (Figure 2). In the ground-state $K_a = 0$ level of $(D_2O)_2$, the two outer levels are split by 1172 MHz in the lower acceptor tunneling component and 1083 MHz in the upper component, while the shift of these levels induced by donor tunneling is estimated to be ∼7 MHz.[21] Again, this value is not known precisely because of the selection rules.

Accurate knowlege of these tunneling splittings is ultimately important because they provide a sensitive measure of the potential energy surface. However, with the moderate resolution of our current CRLAS spectrometer (∼1 GHz), we do not expect to resolve the two smaller tunneling splittings. Donor tunneling is not likely to be enhanced by the intramolecular vibrational excitation and should remain well below our present resolution, while the donor−acceptor interchange splitting, which in the ground state is roughly equal to our laser bandwidth, is almost certainly quenched in the excited state, as was observed in the case of $(H_2O)_2$.[11] This excited-state behavior is rationalized by considering that, for the case of exciting a local mode on the acceptor monomer, this motion would require the rapid transfer of the vibrational energy to the other monomer as they exchange donor−acceptor roles. Since there is no obvious mechanism to allow this to occur on the time scale of the tunneling motion, we expect rotational lines of the acceptor antisymmetric band system measured with the present resolution to contain unresolved triplet structure closely resembling that of the ground state.

The present data, however, provide an interesting perspective on the acceptor tunneling, the largest of these splittings. Our analysis takes advantage of the local mode character of the intramolecular vibrational excitation with the assumption that the acceptor tunneling dynamics change very little in the excited state relative to the ground state. This assumption, discussed below, implies that the excited-state K-dependent splitting pattern should closely resemble that of the ground state. This additional constraint removes the linear correlation between the values of the individual splittings within each K_a level obtained from the measured splittings within each rovibrational band, permitting their accurate determination. This type of analysis was not possible in previous studies that accessed intermolecular vibrational modes, which most likely influence the tunneling dynamics rather strongly.[18,19] Nor was this possible in the previous study of the H_2O dimer acceptor stretch,[11] because only one of the two acceptor tunneling doublets was observed in that work.

Experimental Section

The novel IR-CRLAS spectrometer used to obtain the present results has been described in recent publications.[16,17] Briefly, tunable infrared radiation was generated by Raman shifting a Nd:YAG-pumped pulsed dye laser (Lambda Physik, fl3002e). The Raman shifter consisted of a 3.5 m high-pressure multipass cell (Herriot configuration) containing 200 psi of H_2. After 17 passes, the 20−25 mJ/pulse of fundamental radiation (655−680 nm) generated 0.2−0.5 mJ/pulse of infrared (3.6−4.5 μm) in the third Stokes band. This radiation was carefully aligned along the axis of the ringdown cavity, consisting of a pair of highly reflective dielectric mirrors ($R \sim 0.9999$). The light leaving the cavity was focused with a 10 cm lens onto a 0.5 mm diameter liquid N_2-cooled InSb detector, and the resulting signal was amplified by a 1 MHz bandwidth amplifier contained within the detector housing. This signal was then digitized, averaged (20 shots/wavelength), and sent to a computer for least-squares fitting to a first-order exponential decay. The cavity optical transit time divided by the measured decay time yields the per-pass total cavity loss, which is recorded as a function of wavelength.

The water clusters were generated by expanding a mixture of helium and water vapor into a vacuum chamber through a 4 in. pulsed supersonic slit source,[29] which generally produces clusters with rotational temperatures near 5 K. A background pressure of ∼200 mTorr was maintained during the 40 Hz operation of the source by a 2500 cfm Roots pump. To maximize the signal-to-noise ratio, we found it necessary to limit the number of large clusters formed in the expansion. This was done by seeding a higher pressure He/D_2O mixture into a lower pressure pure He flow through a needle valve, allowing precise control over the water concentration in the expansion, while maintaining a high overall source backing pressure of 35 psia.

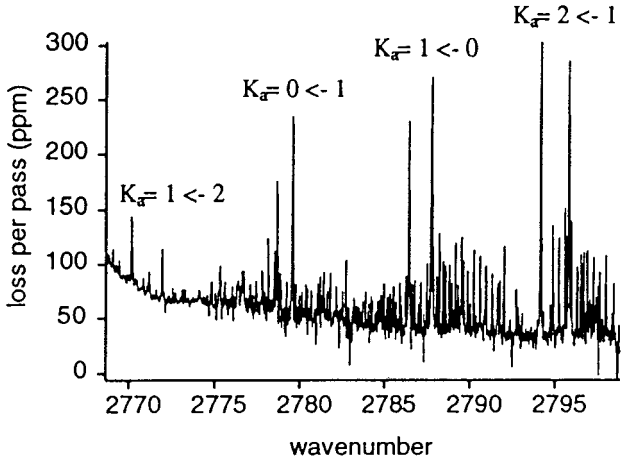

Figure 3. IR-CRLAS spectrum of the $(D_2O)_2$ acceptor antisymmetric stretch. The acceptor tunneling splitting is clearly observed.

The data were wavelength calibrated from D_2O monomer transitions[30] measured simultaneously with the dimer data, which provided a global accuracy of ±300 MHz, while the relative line position accuracy is estimated to be about ±150 MHz. All of the data presented below have been baseline subtracted, which was necessary to remove oscillations in the baseline resulting from a weak coupling between the ringdown cavity and the mirror substrates. This coupling increased the noise level in the scans, most notably with respect to the monomer transitions, which were measured in the background gas even with the source shut off. Because the baseline oscillations tended to drift in frequency slightly over time (presumably from thermal drift of the mirror substrate thickness), the monomer transitions did not generally coincide exactly between the signal and background scans. The decending lines in the baseline (see below) result from this effect.

Results

Under the experimental conditions outlined above, a typical CRLAS spectrum of the 2780 cm^{-1} region is presented in Figure 3. As shown below, these features can be assigned to the acceptor antisymmetric stretch of the D_2O dimer. In all, we have located 10 subbands, clearly belonging to a perpendicular vibrational band system, in which each transition is doubled via acceptor tunneling. Each subband has a strong unresolved Q branch, with well-resolved P and R branches. As expected, most of these lines exhibit partially resolved substructure resulting from the triplet splitting arising from the two other tunneling motions. All of the observed transitions are summarized in Figure 4. We have used the fact that the A_1 states carry twice the nuclear spin weight of the A_2 states[26] to assign the stronger band of each doublet to the A_1 states. Additionally, this diagram incorporates the adjusted ground-state acceptor tunneling splittings discussed below.

While the overall rotational quantum number assignments are easily obtained by noting the missing low J rotational lines within each band (Figure 5), these assignments, as well as the accuracy of the present data, can be verified by comparing determinable ground-state information with that obtained previously from microwave and far-IR experiments. For example, because the $K_a' = 1 \leftarrow K_a'' = 0$ and the $K_a' = 1 \leftarrow K_a'' = 2$ transitions share common upper states, the sum of the observed acceptor tunneling splittings in these bands is a direct measure of the sum of the ground-state $K_a = 0$ and 2 splittings. In fact, the present value of 92.7(5) GHz agrees well with the microwave value of 92.25 GHz.[22,21] Similarly, averaging the locations of

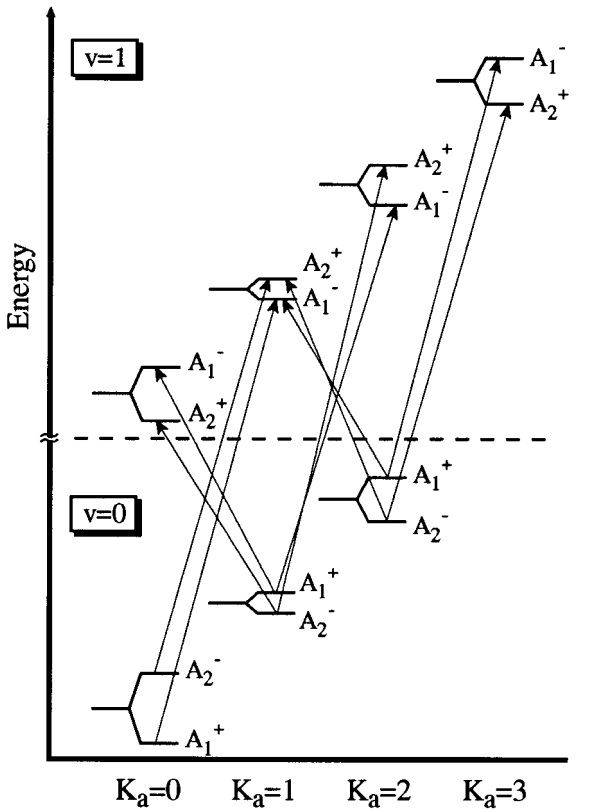

Figure 4. Energy level diagram showing the transistions observed in the present work. In this diagram, the ground-state acceptor tunneling splittings are shown adjusted from their previously reported values based upon the analysis presented here.

the band origins of these tunneling doublets and using the expression[31]

$$^{R}Q_{K-1} - {}^{P}Q_{K+1} = 4(A'' - B'')K \quad (1)$$

yields a ground-state A rotational constant of 125.6(3) GHz. This compares well with 124.9 GHz obtained from the $K_a = 1 \leftarrow 0$ microwave data[21] and 125.8 GHz for $K_a = 2 \leftarrow 1$.[22]

Six of the 10 recorded bands exhibit a sufficient signal-to-noise ratio to permit rotational analysis. As no common upper states were shared among these six bands, they were fit individually using a least-squares algorithm to the standard pseudodiatomic energy level expression

$$\nu = \nu_0 + \bar{B}J(J+1) - D'J^2(J+1)^2 - \bar{B}''J(J+1) + D''J^2(J+1)^2 \quad (2)$$

where $\bar{B} = (B + C)/2$. In all cases, the ground-state $\bar{B}$ constant was first included as a fitted parameter to ensure that the known value could be reproduced within the statistical uncertainty of the fit and was then fixed at the microwave value to more accurately determine the upper state constants. The corrections for asymmetry determined from the microwave data were included for the ground-state $K_a = 1$ levels (not shown in eq 2), but not for the excited-state levels because the Q branches were unresolved and therefore could not included in the fits. This effectively adds a factor of $(B - C)/8$ to the determined value of $\bar{B}$ in the upper state $K_a = 1$ level. Thus, the reported values are "effective" rotational constants. The effect of asymmetry in $K_a = 2$ is expected to be very small, such that the exclusion of this correction should produce a negligible effect for these levels. Finally, the upper state distortion

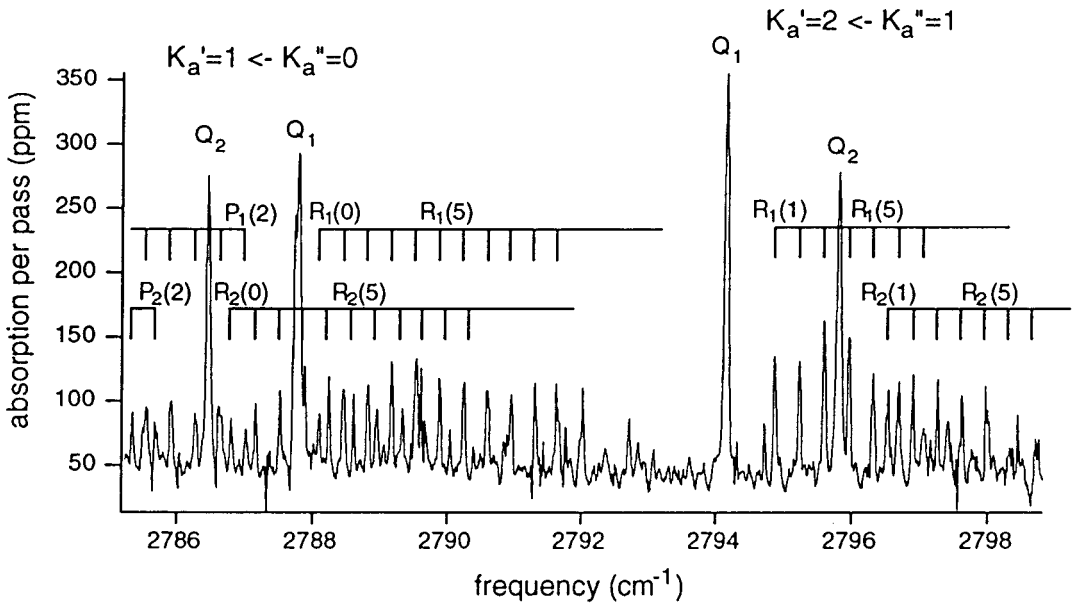

Figure 5. Enlarged view of the spectrum displayed in Figure 3. The rotational line assignments are shown.

TABLE 1: Molecular Constants Obtained from Fitting the Present Data to Eq 1

symmetry	A_1		A_2
band origin		2783.14(2)	
A''		4.190	
A'		4.14(1)	
$(B+C)''/2$			
$K_a=0$	0.18108		0.18108
$K_a=1$	0.18110		0.18102
$K_a=2$	0.18085		0.18094
$(B+C)'/2$			
$K_a=0$	0.1815(1)		0.1813(1)
$K_a=1$	0.1806(1)		0.1811(1)
$K_a=2$	0.1811(1)		0.1803(3)
D		1.2×10^{-6}	

[a] All constants are given in cm^{-1}. The ground-state constants are from refs 21 and 22.

constants were fixed at the ground-state values because we lacked the resolution to determine these constants accurately. In total, 73 lines were fit, producing the molecular constants listed in Table 1. It is interesting to note (Figure 5) the reduction of the P-branch intensity in the $\Delta K = +1$ bands predicted by the Hönl−London factor[31] is particularly apparent in the $K_a' = 2 \leftarrow K_a'' = 1$ bands. Very few P-branch lines could be obtained for these bands because of this effect, slightly reducing the precision of the fitted constants for these bands. Also, the appropriate upper state formula analogous to (1) was used to determine the value of A'.

Perhaps the most interesting insights revealed by the present data concern the acceptor tunneling splittings. For the time being, let us assume that the ground- and excited-state acceptor tunneling splitting patterns are in fact nearly identical (aside from a global inversion of the splitting pattern arising from a change to the total wave function by an antisymmetric rather than symmetric vibrational wave function). A $K_a'' = 0$ splitting of ca. 55 GHz is the only value that satifies this condition within the constraints imposed by the measured splittings within each band and produces the energy level diagram in Figure 4. Interestingly, the resulting splittings fit well to a cosine pattern in both the upper and lower states (Figure 6). The extrapolated periodicity in K_a in both states is ~3.2. In fact, the best simultaneous fit of both tunneling patterns to cosine waves

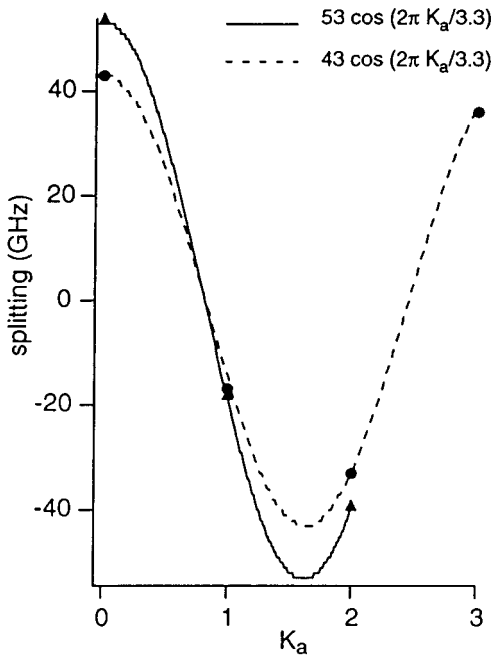

Figure 6. The present description of the tunneling splittings produces upper state (dashed line) and lower state (solid line) splitting patterns that vary cosinusoidally with the K_a quantum number with the same periodicity. This periodicity is consistent with the "methylamine-like" tunneling pathway and lends strong support to the results from a previous local-IAM analysis of $(H_2O)_2$ data. The symbols correspond to the splittings shown in Figure 4 (see text for details).

ranging near this periodicity occurs for a $K_a'' = 0$ splitting of 54 GHz.

This type of K dependence is common in internal rotation/barrier tunneling problems, where the Hamiltonian is described by Mathieu's equation.[28] The periodicity arises from the coupling of the angular momentum generated by the tunneling motion to that from the overall rotation of the cluster. For the simple case of hindered torsional motions in symmetric rotors (the water dimer is near-prolate), the periodicity is a direct measure of the moment of inertia of the internal rotor (I_1), as given by the equation $\Delta K = nI/I_1$, where n represents the number of equilibrium positions. The fact that the periods in both states

are similar is consistent with this picture, while the smaller amplitude in the excited state relative to that of the ground state might be indicative of a slightly higher tunneling barrier in the excited state. The moment of inertia of the internal rotor about the *A*-axis would be 2.6 amu Å^2 within this description. For purposes of comparison, the $(D_2O)_2$ principal axis moments of inertia are $I_A \sim 4.2$ amu Å^2 and $I_B \sim 90$ amu Å^2. Note that the internal rotor inertia constitutes a significant fraction of the *A*-axis inertia, which is more consistent with the methylamine tunneling path than with the conceptually simpler acceptor $\hat{c}_2$ rotation pathway.

Discussion

While a self-consistent picture of the acceptor tunneling splittings emerges from the above considerations, the validity of the underlying assumption, that the splittings are similar in the upper and lower vibrational states, is supported by the following arguments. For the case of the H_2O dimer, the acceptor antisymmetric stretch was the only one of three IR modes measured (and the only one centered on the acceptor monomer) that did not rapidly predissociate the cluster.[11] This implies a relatively weak coupling between this vibrational mode and the hydrogen bond. Furthermore, the shift in frequency of this vibration from the free monomer frequency is less than 0.3%, also indicative of a very small influence on this mode from the hydrogen bond. As this apparently weak coupling to the H bond is not likely to strongly affect the torsional and wagging motions along this bond associated with the acceptor tunneling pathway, it is reasonable to invoke an adiabatic separation between this vibrational mode and motion along the tunneling coordinate. Similarly, the upper state vibrational frequency of 2783 cm^{-1} should produce an averaged symmetric structure on the time scale of the much slower 1−2 cm^{-1} tunneling frequency, effectively preserving the necessary symmetry for the tunneling motion to take place.

The present results are in good agreement with theoretical calculations using a generalized internal axis model (IAM).[25,26] Within this model, these splittings are predicted to follow the relation $(-1)^K \cos(2K\phi_4)$. Using the RWK2 potential energy surface, ϕ_4 was then calculated to be about 222°, giving a periodicity of $\Delta K \sim 3.6$. This value should be very sensitive to the specific tunneling pathway and in this case is consistent with the methylamine-like pathway found from theoretical calculations.[5,26] While this formalism was specifically developed to address cases of high barrier tunneling, it has been extended to include the case of the water dimer (local IAM).[25] Nevertheless, it is less likely to fail for $(D_2O)_2$ than $(H_2O)_2$, because of the significantly lower acceptor tunneling frequency. Previous analysis of $(H_2O)_2$ data within the local IAM framework obtained $\phi_4 \approx 210°$, in reasonable agreement with the predicted value from the RWK2 surface of 222°. The present data agree somewhat better with the predicted value, producing a value of 215°. We should point out that the present results were derived under a different set of assumptions than previous results relying on the IAM model, and thus the consistency of these results provides strong support for the conclusions of these previous studies.

To arrive at the energy level diagram in Figure 4, we made the assumption that the splitting pattern in the excited state does not vary significantly from that of the ground state. Imposing this constraint removes the linear correlation between the measured splittings that results from measuring only the sum or the difference of the upper and lower state splittings, but never the individual splittings themselves. We have argued that, based on the apparent adiabatic separation between the acceptor antisymmetric stretch and the tunneling motion, this assumption should be valid and should therefore lead to reasonable estimates of the tunneling splittings. These results, while not entirely rigorous, are consistent with expectations and previous results and will hopefully result in an improved understanding of the acceptor tunneling dynamics.

Acknowledgment. This work was supported by the AFOSR (Grant #F49620-96-1-0411) and the National Science Foundation (Grant #CHE-9424482). We also wish to thank the Y. T. Lee Research Group for loaning to us the Raman shifter used in these studies.

References and Notes

(1) Liu, K.; Cruzan, J. D.; Saykally, R. J. *Science* **1996**, *271*, 929−933.
(2) Brown, M. G.; Viant, M. R.; Saykally, R. J. Far Infrared Laser VRT Specrtoscopy of Water Clusters. *Proceedings of the NATO-Advanced Study Institute Conference on Recent Theoretical and Experimental Advances in Hydrogen Bonded Clusters, 1997, Heraklion, Crete, Greece*.
(3) Gruenloh, C.; Carney, J.; Arrington, C.; Zwier, T. S.; Fredericks, S. Y.; Jordan, K. D. *Science* **1997**, *276*, 1678−1681.
(4) Xantheas, S. S. *J. Chem. Phys.* **1995**, *102*, 4505−4517.
(5) Wales, D. J. Rearrangements and Dynamics of Water Clusters. In *Advances in Molecular Vibrations and Collision Dynamics*; Bowman, J., Ed., in press.
(6) Gregory, J. K.; Clary, D. C.; Liu, K.; Brown, M. G.; Saykally, R. J. *Science* **1997**, *275*, 814.
(7) Leforestier, C.; Braly, L. B.; Liu, K.; Elrod, M. J.; Saykally, R. J. *J. Chem. Phys.* **1997**, *106*, 8527.
(8) Huisken, F.; Kaloudis, M.; Kulcke, A. *J. Chem. Phys.* **1996**, *104*, 17−25.
(9) Page, R. H.; Frey, J. G.; Shen, Y. R.; Lee, Y. T. *Chem. Phys. Lett.* **1984**, *106*, 373−376.
(10) Vernon, M. F.; Krajnovich, D. J.; Kwok, H. S.; Lisy, J. M.; Shen, Y. R.; Lee, Y. T. *J. Chem. Phys.* **1982**, *77*, 47−57.
(11) Huang, Z. S.; Miller, R. E. *J. Chem. Phys.* **1989**, *91*, 6613−6631.
(12) Reimers, J. R.; Watts, R. O. *Chem. Phys.* **1984**, *91*, 201.
(13) Fredin, L.; Nelander, B.; Ribbegard, G. *J. Chem. Phys.* **1977**, *66*, 4065.
(14) Brentwood, R. M.; Barnes, A. J.; Orville-Thomas, W. J. *J. Mol. Spectrosc.* **1980**, *84*, 391.
(15) Ayers, G. P.; Pullin, A. D. E. *Spectrochim. Acta* **1976**, *32A*, 1629.
(16) Paul, J. B.; Collier, C. P.; Scherer, J. J.; O'Keefe, A.; Saykally, R. J. *J. Phys. Chem. A* **1997**, *101*, 5211−5214.
(17) Scherer, J. J.; Paul, J. B.; O'Keefe, A.; Saykally, R. J. *Chem. Rev.* **1997**, *97*, 25−51.
(18) Busarow, K. L.; Cohen, R. C.; Blake, G. A.; Laughlin, K. B.; Lee, Y. T.; Saykally, R. J. *J. Chem. Phys.* **1989**, *90*, 3937.
(19) Pugliano, N.; Saykally, R. J. *J. Chem. Phys.* **1992**, *96*, 1832.
(20) Coudert, L. H.; Hougen, J. T. *J. Mol. Spectrosc.* **1990**, *139*, 259−277.
(21) Karyakin, E. N.; Fraser, G. T.; Suenram, R. D. *Mol. Phys.* **1993**, *78*, 1179−1189.
(22) Zwart, E.; Meulen, J. J. t.; Meerts, W. L. *Chem. Phys. Lett.* **1990**, *173*, 115.
(23) Zwart, E.; Meulen, J. J. t.; Meerts, W. L.; Coudert, L. H. *J. Mol. Spectrosc.* **1991**, *147*, 27−39.
(24) Dyke, T. R. *J. Chem. Phys.* **1976**, *66*, 492.
(25) Hougen, J. T. *J. Mol. Spectrosc.* **1985**, *114*, 395−426.
(26) Coudert, L. H.; Hougen, J. T. *J. Mol. Spectrosc.* **1988**, *130*, 89−119.
(27) Smith, B. J.; Swanton, D. J.; Pople, J. A.; III, H. F. S.; Radom, L. *J. Chem. Phys.* **1990**, *92*, 1240−1247.
(28) Townes, C. H.; Schawlow, A. L. *Microwave Spectroscopy*; Dover Publications: New York, 1975.
(29) Liu, K.; Fellers, R. S.; Viant, M. R.; McLaughlin, R. P.; Brown, M. G.; Saykally, R. J. *Rev. Sci. Instrum.* **1996**, *67*, 410−416.
(30) Papineau, N.; Flaud, J.-M.; Camy-Peyret, C.; Guelachvili, G. *J. Mol. Spectrosc.* **1981**, *87*, 219−232.
(31) Herzberg, G. *Infrared and Raman Spectra of Polyatomic Molecules*, 1st ed.; Van Nostrand Reinhold: New York, 1945; Vol. 2.